European Journal of Histochemistry 2025; volume 69:4158

Adipose-derived stem cells promote the recovery of intestinal barrier function by inhibiting the p38 MAPK signaling pathway

Mei Yang,[1] Wangbin Xu,[2] Chaofu Yue,[1] Rong Li,[1] Xian Huang,[1] Yongjun Yan,[1] Qinyong Yan,[1] Shisheng Liu,[1] Yuan Liu,[1] Qiaolin Li[1]

[1]Department of Critical Care Medicine, The Qujing No.1 People's Hospital, Qujing
[2]Department of Critical Care Medicine, First Affiliated Hospital of Kunming Medical University, Kunming, China

ABSTRACT

Intestinal barrier damage causes an imbalance in the intestinal flora and microbial environment, promoting a variety of gastrointestinal diseases. This study aimed to explore the mechanism by which adipose-derived stem cells (ADSCs) repair intestinal barrier damage. The human colon adenocarcinoma cell line Caco-2 and rats were treated with lipopolysaccharide (LPS) to establish *in vitro* and *in vivo* models, respectively, of intestinal barrier damage. The expression of inflammatory cytokines (TNF-α, HMGB1, IL-1β and IL-6), antioxidant enzymes (iNOS, SOD and CAT), and oxidative products (MDA and 8-iso-PGF2α) was detected using ELISA kits and related reagent kits. Apoptosis-related proteins (Bcl-2, Bax, Caspase-3 and Caspase-9), tight junction proteins (ZO-1, Occludin, E-cadherin, and Claudin-1) and p38 MAPK pathway-associated protein were detected by Western blotting. In addition, cell viability and apoptosis was determined by a CCK-8 kit and flow cytometry, respectively. Cell permeability was assayed by the transepithelial electrical resistance value and FITC-dextran concentration. The homing effect of ADSCs was detected by fluorescence labeling, and intestinal barrier tissue was observed by HE staining. After ADSC treatment, the level of phosphorylated p38 MAPK protein decreased, the expression of inflammatory factors, oxidative stress and cell apoptosis decreased, the expression of tight junction proteins increased, and cell permeability decreased in Caco-2 cells stimulated with LPS. In rats, ADSCs are directionally recruited to damaged intestinal tissue. ADSCs significantly decreased the levels of D-lactate, diamine oxidase (DAO) and FITC-dextran induced by LPS. ADSCs promoted tight junction proteins and inhibited oxidative stress in intestinal tissue. These effects were reversed after the use of a p38 MAPK activator. ADSCs can be directionally recruited to intestinal tissue, upregulate tight junction proteins, and reduce apoptosis and oxidative stress by inhibiting the p38MAPK signaling pathway. This study provides novel insights into the treatment of intestinal injury.

Key words: intestinal barrier damage; ADSCs; p38 MAPK; oxidative stress; apoptosis.

Correspondence: Mei Yang, Department of Critical Care Medicine, The Qujing No.1 People's Hospital, No. 1, Yuanlin Road, Qilin District, Qujing City, Yunnan 655000, China. E-mail: ym13987413637@163.com

Contributions: MY, WX, study design, experiments, interpretation of results, writing, manuscript revision; CY, RL, XH, YY, animal experiments; QY, SL, YL, data analysis; QL, study design and funding support. All authors contributed to the study's preparation and design and agree with the content of the manuscript.

Conflict of interest: the authors declare no conflict of interest.

Ethical approval: this study was approved by the Animal Ethics Committee of Kunming Medical University Animal Center (Approval no. SYXK-K2020-0006).

Availability of data and materials: the data used to support the findings of this study are available from the corresponding author upon reasonable request.

Funding: this work was supported by the Yunnan Provincial Science and Technology Plan Project (No. 202101AY070001-228).

Introduction

The intestinal barrier is the first barrier to prevent the passage of luminal contents into the body.[1] There are many causes of intestinal barrier damage, such as hypoxia, ischemia, increased intestinal permeability, and bacterial translocation.[2,3] An increase in intestinal permeability mainly manifests as downregulation of B-cell lymphoma 2 (Bcl-2) protein expression and a reduction in the expression of tight junction proteins such as claudin-2, claudin-5, and zonula occludens (ZO)-1.[1] If intestinal barrier damage cannot be repaired in time, it will cause intestinal dysfunction, which will lead to extensive inflammation and multiple organ failure.[4,5] Understanding the pathogenesis of the intestinal mucosal barrier and identifying new therapeutic methods are highly important for preventing intestinal barrier damage. Mitogen-activated protein kinase p38 (p38MAPK) is often activated by phosphorylation of the Thr-X-Tyr sequence by upstream MAPK. P38 MAPK is involved in the inflammatory response, stress response, apoptosis and autophagy.[6,7] In recent years, it has been found that P38 MAPK plays an important role in intestinal barrier damage. For example, Gingerol exerts protective effects against ischemia/reperfusion-induced intestinal mucosa injury by inhibiting the formation of ROS and p38 MAPK activation.[8] Icariin and its phosphorylated derivatives regulate the inflammatory response and oxidative stress in intestinal epithelial cells by inhibiting the expression of p38 MAPK.[9] In another study, it was found that upregulation of tight junction proteins by p38 MAPK/p53 inhibition leads to a reduction in injury to the intestinal mucosal barrier.[10] Therefore, it is novel and meaningful to explore the specific mechanism by which the p38 MAPK pathway affects intestinal barrier injury.

Adipose-derived stem cells (ADSCs) are mesenchymal stem cells that have immune properties, can prevent severe rejection, and can be cultured stably *in vitro*.[11] In a mouse model of diabetic nephropathy, ADSCs were found to attenuate the symptoms of diabetic nephropathy by promoting autophagy and inhibiting apoptosis.[12] In addition, studies have reported that ADSCs have enormous potential in the treatment of intestinal-related diseases.[13,14] Thus, exploring the mechanism by which ADSCs regulate intestinal barrier damage will provide a more theoretical basis for the treatment of intestinal barrier damage. ADSCs have been shown to have a regulatory effect on the p38MAPK signaling pathway. Wang reported that ADSCs can inhibit Jurkat cell proliferation through the TGF-β1-p38 signaling pathway.[15] Exosomes from ADSCs improve liver fibrosis by repressing the activation of the p38 MAPK/NF-κB pathway,[16] and ADSCs suppress hypertrophic scar fibrosis *via* the p38/MAPK signaling pathway.[17] However, it is unclear whether ADSCs can promote the recovery of intestinal barrier damage by regulating p38 MAPK. Hence, this study aimed to explore the ability of ADSCs to regulate the p38MAPK signaling pathway and thus affect intestinal barrier damage.

Materials and Methods

Cell culture

The human colon adenocarcinoma cell line Caco-2 (purchased from the cell bank of the Shanghai Academy of Sciences, Chinese Academy of Sciences (Shanghai, China), and introduced by ATCC) was selected for the experiment. The cells were maintained at 37°C and 5% CO_2 in DMEM supplemented with 10% (v/v) fetal bovine serum (FBS) and 1% penicillin/streptomycin. After two to three generations, when the confluence degree reached more than 80%, the cells were collected for follow-up experiments.

Lipopolysaccharide exposure to establish a cell model of intestinal barrier damage

An intestinal barrier injury cell model was established by adding LPS. The specific steps were described by Panaro *et al.*[18] Briefly, Caco-2 cells were inoculated at 4 × 10^5/well. Cells in the model group were treated with *Salmonella enterica* serotype *typhimurium* LPS (Sigma-Aldrich, St. Louis, MO, USA) for 48 h. The ADSC group was also treated with LPS for 48 h, and 4 × 10^5 ADSCs were immediately added. HY-N0674A (p38 MAPK activator, MedChemExpress, Monmouth Junction, NJ, USA) and SB203580 (p38 MAPK inhibitor, Yeasen Biotech, Shanghai, China) were used when the ADSCs were added according to the manufacturer's instructions.

Transepithelial electrical resistance measurements

The transepithelial electrical resistance (TEER) was detected using a microcellular resistance system. The cells were placed in an incubator at room temperature for 30 min. After the culture medium was removed, new cell culture medium was added, and the TEER was measured. TEER value ($\Omega.cm^2$) = (sample resistance value-blank control value) × membrane surface area of the Transwell chamber.

Cell permeability detection

Caco-2 cells (4×10^4 cells/well) were inoculated into the upper chamber of a Transwell insert (Corning, Corning, NY, USA) and they were cultured for 24 h. Then, FITC-dextran (10 mg/mL; MedChemExpress) was added to the upper chamber. Two hours later, the cell culture medium was collected, and the absorbance value was detected by a microplate reader (Thermo Fisher, Waltham, MA, USA).

CCK8 assay

Caco-2 cells (5×10^3 cells/well) were cultured at 37°C in a 96-well plate. After treatment, 20 μL of CCK-8 reagent was added and incubated for 2 h. Finally, the absorbance at 450 nm was measured by an enzyme marker (ELX800, BioTeK, Biotek Winooski, VT, USA).

Flow cytometry

Cell apoptosis was identified by using a propidium iodide (PI)-Annexin V Apoptosis Detection Kit (BD Biosciences, San Jose, CA, USA) according to the manufacturer's instructions. A total of 1×10^4 cells were collected by flow cytometry (CyFlow Cube 8, GENETIMES, Shanghai, China) for apoptosis detection and analysis. The experiments were divided into three parallel groups and repeated three times.

Immunofluorescence

In a culture plate, the slide with the cells was washed with PBS 3 times. The cells were fixed with 4% paraformaldehyde at room temperature for 15 min, permeabilized and then incubated with a sufficient dilution of anti-ZO-1 (1:1000, Abcam, Cambridge, MA, USA) at 4°C overnight. The fluorescent secondary antibody (from Invitrogen, diluted at 1:500) was incubated at room temperature for 1 h. DAPI was added and incubated for 5min in dark light, and the samples were nucleated. After staining with DAPI, the tablets were sealed with a sealing solution containing an anti-fluorescence quencher, and photos were taken by fluorescence microscope (400857, NiKon, Tokyo, Japan) using a 20× objective. For each sample, three microscope fields were considered. Negative controls were included where cells were incubated without the primary antibody but with all other reagents. The relative fluorescence density was calculated to evaluate the immunolabelling. We used

ImageJ software to accurately measure the fluorescence intensity and perform calculations for relative fluorescence density.

Rat ADSC culture and labeling

ADSCs extracted from rat groin fat were purchased from Cyagen Biotechnology (Yangzhou, China). The cells were cultured according to the manufacturer's instructions. Flow cytometry analysis revealed that CD29, CD90, and CD44 were positively expressed, while CD45 was negatively expressed in the ADSCs.

Establishment of a rat model of intestinal barrier damage

Six- to eight-week-old SD rats were provided and approved for use by the Experimental Animal Center of Kunming Medical University. The animals were maintained on a 12 h light-dark cycle and given enough food. The animal model was established by gavage administration of LPS dissolved in normal saline every 48 h for 2 days (2 times in total, 4 mg/kg). ADSC-treated rats were injected with 1×10^6 ADSCs through the tail vein on the 3rd day. HY-N0674A and SB203580 were injected intraperitoneally according to the manufacturer's instructions when the ADSCs were injected. On the 6th day, the rats were euthanized, and serum and intestinal tissue were collected for subsequent experiments. This study was approved by the Animal Ethics Committee of Kunming Medical University Animal Center (Approval no. SYXK-K2020-0006).

Measurement of D-lactate, DAO and endotoxin levels in the serum

The serum was collected at the end of the experiment and then stored at −80°C. The serum levels of D-lactate (AF7304-SP) and DAO (8298-AO-010) were determined using an enzymatic spectrophotometric assay with reagent kits according to the manufacturer's protocols (Sigma–Aldrich, St. Louis, MO, USA). The serum levels of endotoxin (YX1214) were determined using a Limulus Amebocyte Lysate Assay kit (Shanghai Biochemical Co., Ltd., Shanghai, China) according to the manufacturer's protocols.

Analysis of indicators related to oxidative stress and inflammatory factors

Cell lysates, rat intestinal tissue lysates and serum were collected after different treatments according to the experimental requirements. Inflammatory cytokines (TNF-α, HMGB1, IL-1β and IL-6) were detected using ELISA kits (Solarbio, Beijing, China). The activities of antioxidant enzymes (iNOS, SOD and CAT) and oxidative products (MDA and 8-iso-PGF2α) were detected using related reagent kits (COIBO BIO, Shanghai, China) according to the manufacturer's protocols.

Western blot analysis

Total protein was extracted from cells and rat intestinal tissue. Total protein was separated by SDS-PAGE and transferred to a PVDF membrane (Bio-Rad, Hercules, CA, USA). After blocking in 2% BSA, the membranes were incubated with primary antibodies (Abcam, UK): p38 MAPK (1:1000), JNK (1:1000), ERK (1:1000), MYPT-1 (1:1000), ZO-1 (1:2000), Occludin (1:2000), E-Cadherin (1:1000), Claudin-1 (1:2000), Bcl-2 (1:1000), Bax (1:2000), Caspase-3 (1:2000), Caspase-9 (1:2000) at 4°C overnight and then with the corresponding HRP-conjugated secondary antibodies for 1 h at room temperature. The results were then visualized with an enhanced chemiluminescence detection system, and GAPDH served as the loading control. The band intensity was quantified by ImageJ. All antibodies were obtained from Abcam and used according to the manufacturer's instructions.

Detection of ADSC homing

ADSCs in the logarithmic growth phase were made into single-cell suspensions, and the prepared dye solution (CFSE) was added to the cell suspension for incubation at an appropriate temperature. The CFSE (Lianke Biology, Hefei, China) reagents were used according to the manufacturer's instructions. The stained cells were then stored for subsequent experiments. The rats were injected with 1×10^6 ADSCs stained with CFSE through the tail vein. Liver, kidney and intestinal tissues were collected and cut into tissue sections after fixation for 48 h. After the slices were rinsed with PBS, the sections were counterstained with DAPI at room temperature. Finally, seal the slide with a coverslip. The distribution of the stained ADSCs in the tissue was analyzed under a fluorescence microscope (400857, Nikon) using a 20× objective lens. For each sample, five random microscope fields were selected. Immunolabeling is assessed by measuring the fluorescence intensity of the ADSC-specific immunofluorescence signal in each selected microscope field of view using ImageJ software.

Hematoxylin and eosin (H&E) staining

Intestinal tissue samples were isolated and treated with 4% paraformaldehyde for one day at 4°C. Tissues were rinsed with running water, dehydrated with 70%, 80%, and 95% ethanol, and treated with 100% ethanol. Then, the ethanol was removed with xylene. The tissue samples were routinely embedded, sectioned and stained with H&E (Merck, Germany), sealed with a coverslip, and observed with an optical microscope to record the images.

Statistical analysis

The experimental data were statistically analyzed using GraphPad Prism 7.0 (La Jolla, CA, USA). The cell experiments were performed in triplicate, with each parallel experiment repeated at least 3 times. The animal experiments included 5 parallel experiments, each of which was repeated at least 3 times. The data are expressed as the mean ± SD. ANOVA was used to measure differences between groups. A p-value <0.05 was considered to indicate statistical significance.

Results

Identification of ADSCs

ADSCs were cultured for 2-3 generations, and their cell surface markers were detected by flow cytometry. The results showed that the cell surface contained CD29, CD44 and CD90, which were typical ADSCs surface markers, and no CD45 antibody was found (Figure 1A). Then, the cells were subjected to three-line differentiation culture, and the results showed that the ADSCs could be stained with red oil drops by oil red O staining solution. Second, the cells were stained with Alizarin red to form red calcium nodules under a microscope. In addition, patches of blue cartilage lacunae were observed under a microscope after staining with Alcian blue (Figure 1B). It was confirmed that the above cells met the experimental requirements and could be used for subsequent experiments.

Effects of ADSCs on proliferation and apoptosis of intestinal barrier injury model cell Caco-2

ADSCs also have special functions in regulating cell proliferation and apoptosis. To verify the complex relationship between intestinal barrier damage and abnormal cell apoptosis, Caco-2 cells treated with LPS were used to establish a cell model of intestinal barrier damage. LPS inhibited cell viability and promoted cell

apoptosis in Caco-2 cells; after the addition of ADSCs, cell apoptosis decreased, and cell viability increased (Figure 2 A,B). In addition, LPS increased the expression of Bax, Caspase-3 and Caspase-9 but not Bcl-2. The addition of ADSCs reversed the changes in the expression of the above proteins, suggesting that ADSCs protect Caco-2 cells from LPS-induced cell apoptosis (Figure 2C). Furthermore, the influence of ADSCs on intestinal barrier integrity was investigated. TEER and permeability detection revealed that treatment with LPS inhibited the TEER (Figure 2D) and increased the flux of FITC-dextran (Figure 2E). ADSCs increased the TEER and restrained the flux of FITC-dextran. Furthermore, Western blot and immunofluorescence assays revealed that the levels of the tight junction-associated proteins ZO-1, Occludin, E-cadherin, and Claudin-1 were obviously decreased in the LPS groups. Compared with those in the LPS group, the addition of ADSCs promoted ZO1, Occludin, E-cadherin, and Claudin-1 expression (Figure 2 F,G). Therefore, the application of ADSCs relieved the intestinal barrier damage in LPS-stimulated Caco-2 cells.

Effects of ADSCs on oxidative stress and inflammation in Caco-2 cells

Oxidative stress and the inflammatory response are also considered important triggers of intestinal barrier damage. To determine whether ADSCs are involved in these processes, inflammatory cytokines (TNF-α, HMGB1, IL-1β and IL-6) and the activities of antioxidant enzymes (iNOS, SOD and CAT) and oxidative products (MDA and 8-iso-PGF2α) were detected using ELISA kits and related reagent kits. Compared with those in the NC group, TNF-α, HMGB1, IL-1β, IL-6, MDA and 8-iso-PGF2α were upregulated, while iNOS, SOD and CAT were significantly inhibited in LPS-induced Caco-2 cells, suggesting that oxidative stress and the inflammatory response are closely related to intestinal barrier damage. After coculture with ADSCs, TNF-α, HMGB1, IL-1β, IL-6, MDA and 8-iso-PGF2α were suppressed, while the levels of iNOS, SOD and CAT were significantly increased (Figure 3 A-I). The above results indicated that ADSCs participate in and regulate oxidative stress and inflammation in the intestinal barrier.

Effects of ADSCs on different signaling pathways in Caco-2 cells

Signaling pathways play important roles in cellular metabolism. To explore which signaling pathway has a regulatory function in intestinal barrier damage, several common signaling pathway-related genes, including p38 MAPK, JNK, ERK and MYPT-1, were screened and detected. Analysis of the resulting data revealed that the levels of the phosphorylated proteins p38 MAPK, JNK, ERK and MYPT-1 tended to increase in the LPS group. After coculture with ADSCs, only the levels of the phosphorylated proteins p38 MAPK and ERK were decreased, while the decrease in the p-p38 MAPK level was more obvious (Figure 4). Therefore, the p38 MAPK signaling pathway was selected for subsequent experimental research.

ADSCs inhibited cell apoptosis and restored intestinal barrier integrity by suppressing p38 MAPK

To verify the complex relationship between intestinal barrier damage and p38 MAPK, p38 MAPK activator and p38 MAPK inhibitor were used in Caco-2 cells cultured with ADSCs. ADSCs increased cell viability and inhibited cell apoptosis in LPS-stimulated Caco-2 cells. Compared with those in the LPS+ADSC group, the p38 MAPK activator promoted cell apoptosis while the p38 MAPK inhibitor further inhibited cell apoptosis (Figure 5 A,B). In addition, the p38 MAPK activator increased the expression of Bax, Caspase-3 and Caspase-9 but not Bcl-2 in comparison to that in the LPS+ADSC group. The p38 MAPK inhibitor reversed the decreas-

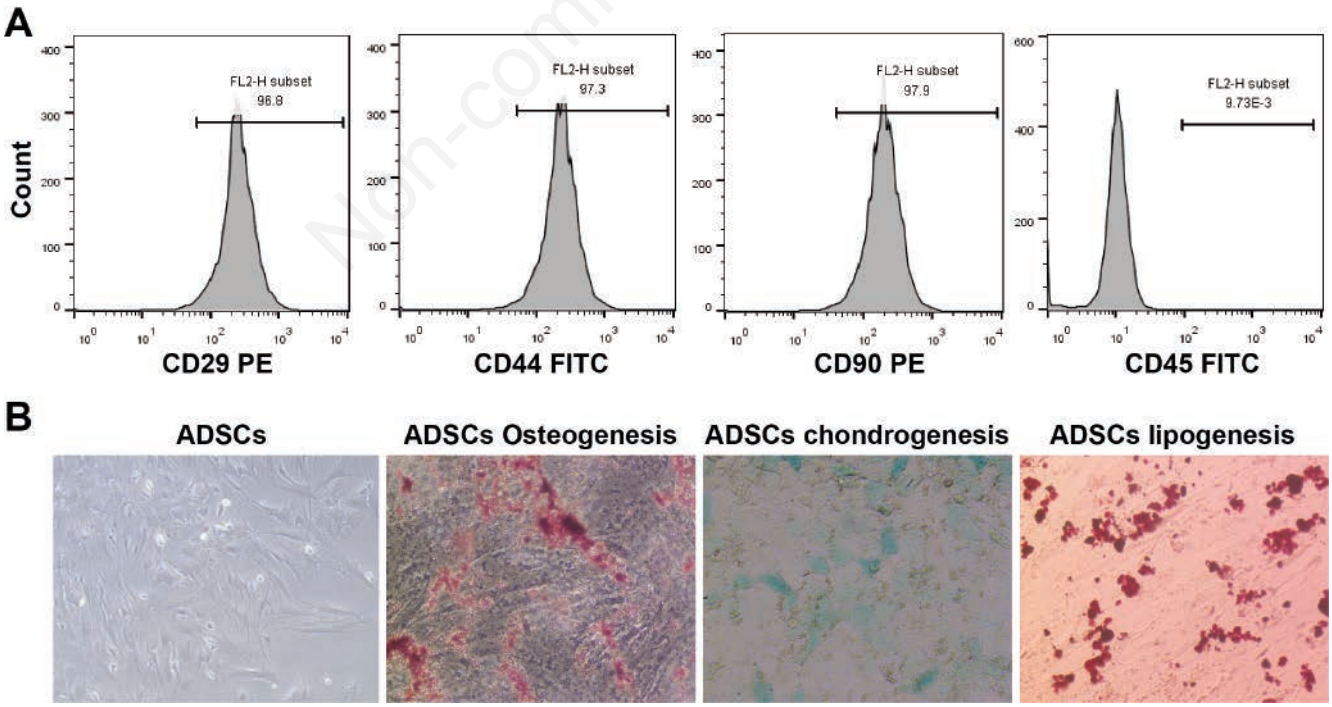

Figure 1. Identification of ADSCs. **A**) ADSC surface markers determined by flow cytometry. **B**) A three-line differentiation test was used to verify ADSCs. (n=3).

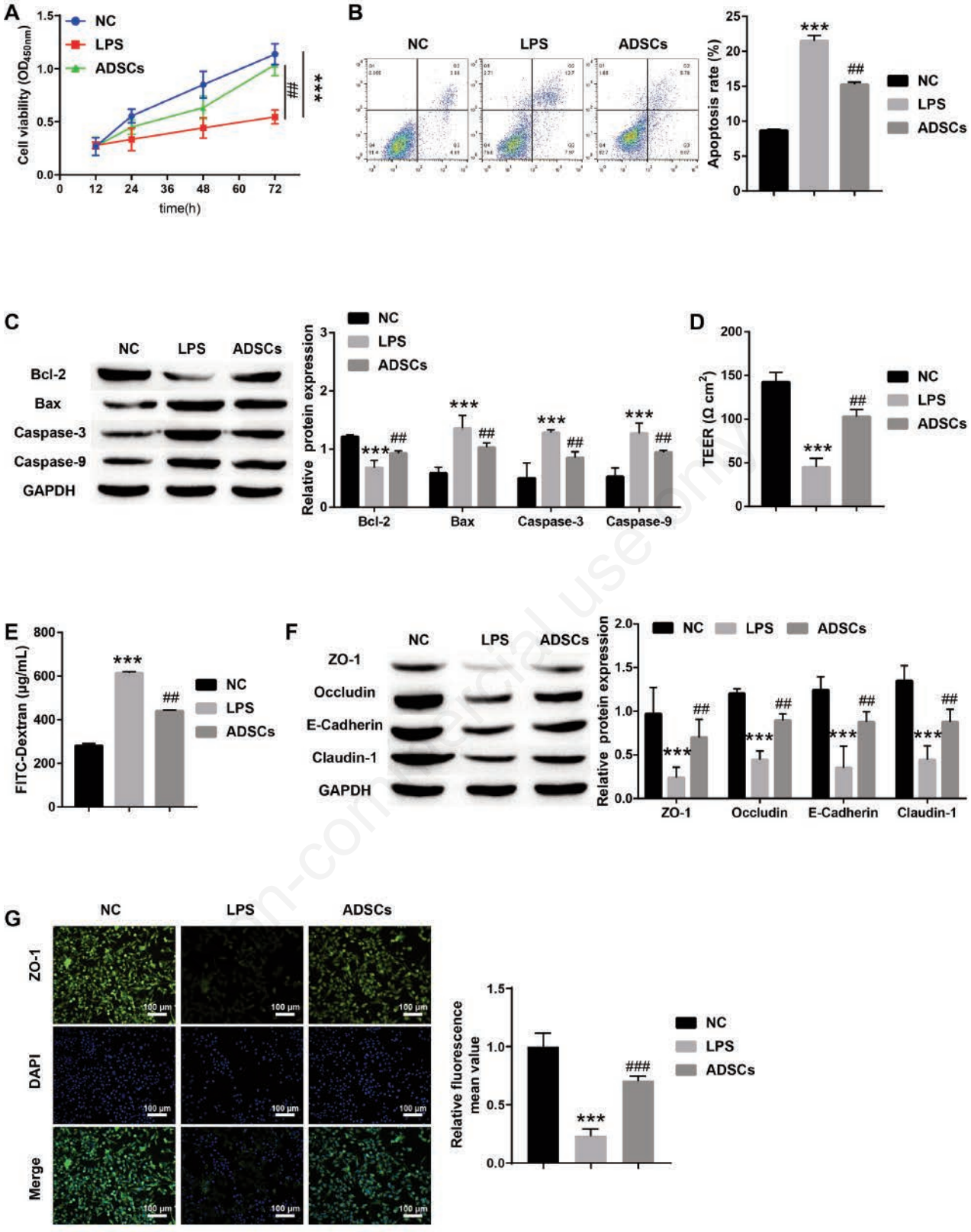

Figure 2. Effect of ADSCs on Caco-2 cell apoptosis and intestinal barrier integrity. **A**) Cell viability was measured by a CCK-8 kit. **B**) Cell apoptosis was tested by flow cytometry. **C**) Apoptosis-related proteins (Bcl-2, Bax, Caspase-3 and Caspase-9) were detected by Western blot. **D**) TEER was detected using a microcellular resistance system. **E**) Cell permeability was assayed by FITC-dextran. **F**) Tight junction proteins (ZO-1, Occludin, E-cadherin, and Claudin-1) were detected by Western blot. G) ZO-1 was observed by immunofluorescence. ***p<0.001 *vs* NC group; ##p<0.01 *vs* LPS group. (n=3). The full-length gel and blot images are available in the Supplementary Figure.

es in the expression of Bax, Caspase-3 and Caspase-9 but not Bcl-2, suggesting that ADSCs protect Caco-2 cells from LPS-induced cell apoptosis by inhibiting p38 MAPK (Figure 5C). Furthermore, the influence of ADSCs and p38 on intestinal barrier integrity was investigated. TEER and permeability detection revealed that ADSCs increased the TEER and restrained the flux of FITC-dextran. The p38 MAPK activator inhibited the TEER values and increased the flux of FITC-dextran, while the p38 MAPK inhibitor further elevated the TEER and restrained the flux of FITC-dextran (Figure 5 D,E). Furthermore, Western blot analysis revealed that the ZO-1, Occludin, E-cadherin, and Claudin-1 levels were obviously increased in the LPS+ADSC group. Compared with those in the LPS+ADSC group, the addition of the p38 MAPK activator inhibited the expression of ZO1, Occludin, E-cadherin, and Claudin-1, while the p38 MAPK inhibitor promoted the expression of the above proteins (Figure 5 F,G). Therefore, the application of ADSCs relieved intestinal barrier damage by suppressing p38 MAPK.

ADSCs inhibited inflammatory and oxidative stress by restraining p38 MAPK

To determine whether ADSCs are involved in oxidative stress and the inflammatory response by p38 MAPK, inflammatory cytokines (TNF-α, HMGB1, IL-1β and IL-6), activities of antioxidant enzymes (iNOS, SOD and CAT) and oxidative products (MDA and 8-iso-PGF2α) were detected using ELISA kits and related reagent kits. Compared with those in the LPS group, the levels of TNF-α, HMGB1, IL-1β, IL-6, MDA and 8-iso-PGF2α were decreased, while the levels of iNOS, SOD and CAT were significantly increased after coculture with ADSCs. After the addition of the p38 MAPK activator, TNF-α, HMGB1, IL-1β, IL-6, MDA and 8-iso-PGF2α were increased, while the levels of iNOS, SOD and CAT were significantly decreased. The p38 MAPK inhibitor and p38 MAPK activator had opposite effects (Figure 6). The above results indicated that ADSCs participate in and regulate oxidative stress and inflammation by restraining p38 MAPK activation in the intestinal barrier.

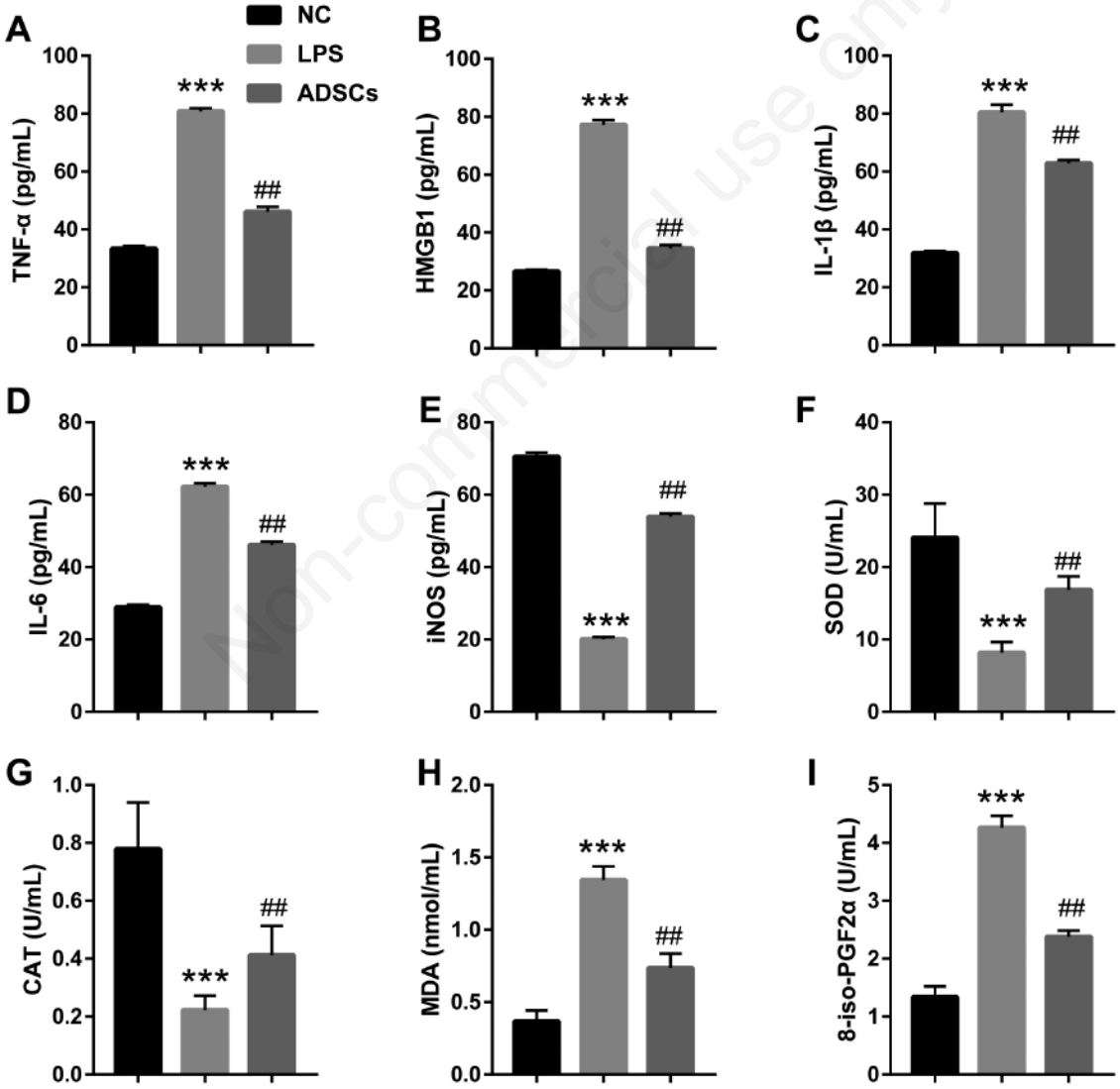

Figure 3. Effects of ADSCs on oxidative stress and inflammation in Caco-2 cells. **A-D**) Inflammatory cytokines (TNF-α, HMGB1, IL-1β and IL-6) were measured by ELISA. **E-G**) Antioxidation enzymes (iNOS, SOD and CAT) were measured by kits. **H-I**) Oxidative products (MDA and 8-iso-PGF2α) were detected by kits. ***p<0.001 *vs* NC group; $^{\#\#}p$<0.01 *vs* LPS group. (n=3).

The recruitment of ADSCs to intestinal tissue alleviates intestinal barrier damage by suppressing p38 MAPK

First, ADSCs were injected into rats (the control group was injected with physiological saline) to detect their localization in different tissues. The results indicated that ADSCs effectively transferred to intestinal tissue rather than to the kidneys or liver (Figure 7A). This, to some extent, confirms the characteristic role of ADSCs in intestinal barrier damage. Next, we constructed a rat model of intestinal barrier damage, and a p38 MAPK activator or inhibitor was used to observe the role of p38 in intestinal barrier repair. The intestinal mucosa of the NC and Sham groups of rats was intact in morphology, with clear villous structures and slightly widened subepithelial spaces at the tips of some villi. However, in the model group, the intestinal mucosal structure was disrupted, with damaged villi and a large amount of epithelial cell shedding. The injection of ADSCs alleviated the intestinal barrier damage, and the p38 MAPK activator weakened the function of the ADSCs. The p38 MAPK inhibitor and p38 MAPK activator had opposite effects (Figure 7B). The levels of D-lactate, DAO and endotoxin were determined in intestinal samples obtained from the portal vein. The levels of D-lactate, DAO and FITC-dextran were significantly greater in the Model group than in the Sham group, indicating that LPS disrupted the integrity of the intestinal mucosal barrier. Treatment with ADSCs significantly decreased the levels of D-lactate, DAO and FITC-dextran. At the same time, treatment with p38 MAPK activators reversed the effects of ADSCs and promoted the levels of these factors, and p38 MAPK inhibitors exhibited the opposite effect of p38 MAPK activators (Figure 7 C-E). In addition, ADSCs promoted ZO-1, Occludin, E-cadherin, and Claudin-1 expression in the model group. The p38 MAPK activator inhibited the increase in these proteins, while the p38 MAPK inhibitor further increased the expression of these proteins (Figure 7F). In addition, ADSCs inhibited the levels of TNF-α, IL-1β and IL-6 in the serum. ADSCs promoted the levels of iNOS, SOD and CAT, suggesting that ADSCs inhibited inflammation and oxidative stress. Furthermore, the p38 MAPK activator reversed the effects of ADSCs on oxidative stress and inflammation, and p38 MAPK inhibitors exhibited the opposite effect of p38 MAPK activators (Figure 7 G-L). These results suggested that the effects of LPS on intestinal injury and mucosal permeability were attenuated by ADSCs, whereas activation of the p38 MAPK signaling pathway promoted further damage to the intestinal mucosa.

Discussion

The intestinal tract is the site with the greatest enrichment of bacteria in the human body.[19] Maintaining the microecological balance and a normal intestinal mucosal mechanical and immune barrier are important conditions for the intestinal mucosa to protect the body from the intestinal contents.[20] However, when the intestinal tract suffers severe pathogenic bacterial invasion or mechanical trauma, the intestinal mucosal barrier will be destroyed, and the body will experience severe adverse reactions, such as inflammatory reactions, multiple organ failure and other common clinical symptoms.[21,22] Therefore, preventing and treating intestinal barrier dysfunction is of great practical significance.

ADSCs are adult stem cells that reside in adipose tissue. They can be recruited in a homing manner to sites of inflammation, where they exhibit powerful immunomodulatory capabilities to promote wound healing and regeneration.[23] ADSCs have been used to treat many diseases. NI *et al.* reported that ADSCs can differentiate into vascular lineages *in vitro* and *in vivo*, participate in vascular remodeling, and can be used to treat cardiovascular diseases.[24] They are also considered to be an important seed cell for bone repair. Second, they can be used for wound repair and regeneration and participate in immune regulation of the body.[25-27] ADSCs are directionally recruited to intestinal tissue through their homing ability and can alleviate inflammatory symptoms in ulcerative colitis model mice.[28] Due to their multiple cellular functions and therapeutic potential in different diseases, ADSCs also have great potential in the repair of intestinal barrier injury. ADSCs also have potential clinical applications in the treatment of intestinal injury. The homing ability of ADSCs to intestinal tissue and its immunomodulatory ability are key factors for their potential clini-

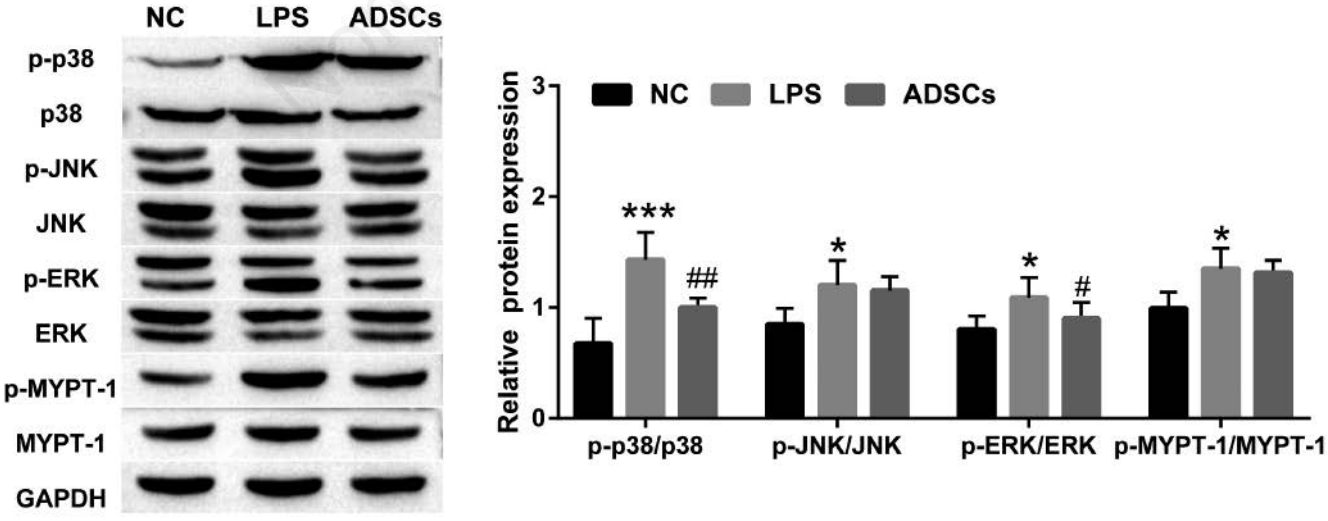

Figure 4. Effects of ADSCs on different signaling pathways in Caco-2 cells. p38 MAPK, JNK, ERK and MYPT-1 were detected by Western blot. *p<0.05, ***p<0.001 *vs* NC group; $^{\#\#}p$<0.01 *vs* LPS group. (n=3). The full-length gel and blot images are available in the Supplementary Figure.

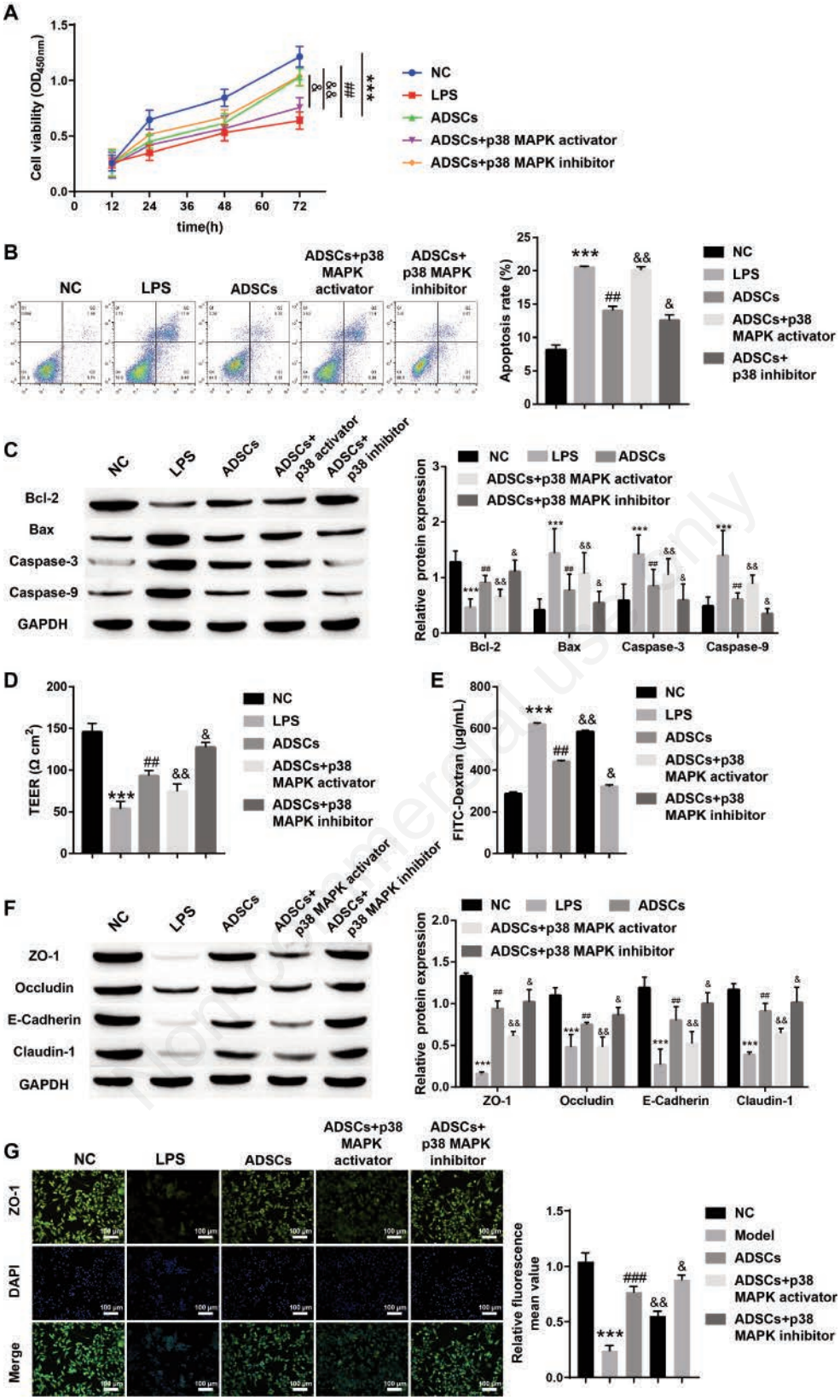

Figure 5. ADSCs inhibited cell apoptosis and restored intestinal barrier integrity by suppressing p38 MAPK. **A**) Cell viability was measured by a CCK-8 kit. **B**) Cell apoptosis was tested by flow cytometry. **C**) Apoptosis-related proteins (Bcl-2, Bax, Caspase-3 and Caspase-9) were detected by Western blot. **D**) TEER was detected using a microcellular resistance system. **E**) Cell permeability was assayed by FITC-dextran. **F**) Tight junction proteins (ZO-1, Occludin, E-cadherin, and Claudin-1) were detected by Western blot. **G**) ZO-1 was observed by immunofluorescence. ***p<0.001 *vs* NC group; $^{\#\#}p$<0.01, $^{\#\#\#}p$<0.001 *vs* LPS group; $^{\&}p$<0.05, $^{\&\&}p$<0.01 *vs* ADSCs group. (n=3). The full-length gel and blot images are available in the Supplementary Figure.

cal applications. Oxidative stress has been proven to be the key pathogenesis of intestinal mucosal dysfunction.[29] In one study, the levels of inflammatory factors, malondialdehyde and oxidative stress-related enzymes in the intestine of uremic rats were detected. The upregulation of the above physiological parameters suggests that kidney diseases can induce intestinal barrier injury and cause systemic inflammation.[30] Apoptosis is another key factor in intestinal mucosal dysfunction. It has been reported that the apoptosis of porcine intestinal epithelial cells exacerbates oxidative damage.[31] Severe acute pancreatitis can cause intestinal barrier damage and then lead to a sudden increase in the expression of Bax/Bcl-2 and other apoptosis-related proteins.[32] In this study, Caco-2 cells treated with LPS were used to establish a cell model of intestinal barrier damage to verify the relationship between intestinal barrier damage and abnormal cell apoptosis or oxidative stress. The results indicated that LPS inhibited cell viability and promoted cell apoptosis. In addition, TNF-α, HMGB1, IL-1β, IL-6, MDA and 8-iso-PGF2α were upregulated, while the levels of iNOS, SOD and CAT were significantly inhibited in LPS-induced Caco-2 cells, suggesting that LPS activated oxidative stress and the inflammatory response. After co-culture with ADSCs, the ADSCs protected Caco-2 cells from LPS-induced cell apoptosis, oxidative stress and inflammation.

Changes in intestinal barrier permeability are one of the major causes of intestinal mucosal barrier damage. Tight junction proteins, including ZO-1, Claudin-1, and Occludin, are important proteins involved in maintaining intestinal mucosal integrity. Decreased expression of these proteins is often a significant marker of intestinal mucosal barrier damage.[33,34] In one study, in a mouse model of intestinal mucosal injury induced by a high-fat diet, intestinal mucosal injury in mice recovered after the expression of ZO-1 was induced by butyrate.[35] The levels of ZO-1, Occludin and Claudin-1 proteins in the ileum of mice with intestinal barrier damage were increased after arbutin treatment, and the expression of p38MAPK signaling pathway proteins was changed.[36] In this work, LPS inhibited the TEER and increased the flux of FITC-dextran. In addition, ZO-1, Occludin, E-cadherin, and Claudin-1 levels were obviously decreased in the LPS groups. The addition of ADSCs reversed the above results, as ADSCs can reshape the healthy intestinal barrier by upregulating the expression of tight junction proteins and mediating intestinal barrier integrity. The activation of the p38 MAPK signaling pathway contributes to the occurrence of inflammation and apoptosis, and it has significant regulatory functions not only in tumor-related diseases but also in the development of inflammatory diseases.[37,38] It has been proven that activation of the p38 MAPK signaling pathway promotes intestinal barrier dysfunction by inducing inflammatory and apoptotic responses.[39] In the intestinal tissue of ulcerative col-

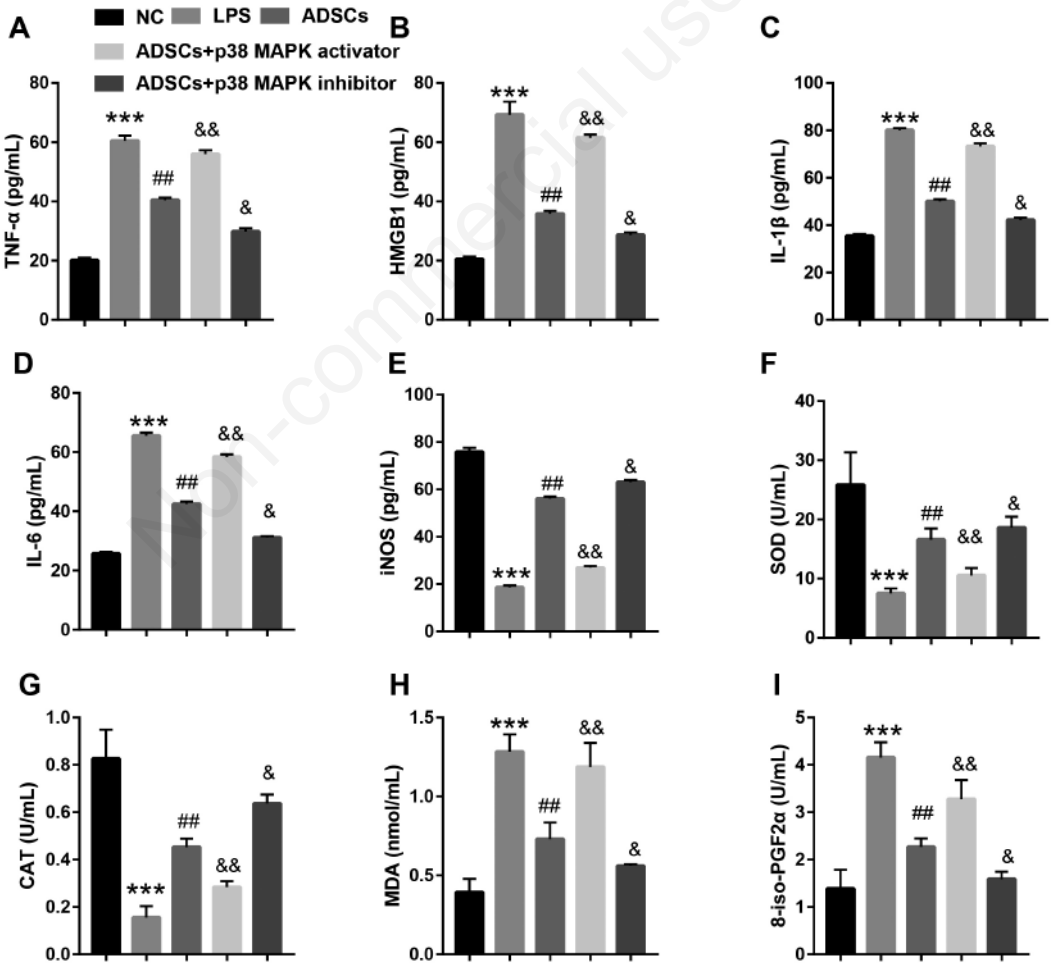

Figure 6. ADSCs inhibited inflammatory and oxidative stress by restraining p38 MAPK. **A-D**) Inflammatory cytokines (TNF-α, HMGB1, IL-1β and IL-6) were measured by ELISA. **E-G**) Antioxidation enzymes (iNOS, SOD and CAT) were measured by kits. **H-I**) Oxidative products (MDA and 8-iso-PGF2α) were detected by kits. ***p<0.001 *vs* NC group; $^{\#\#}p$<0.01 *vs* LPS group; $^{\&}p$<0.05, $^{\&\&}p$<0.01 *vs* ADSCs group. (n=3).

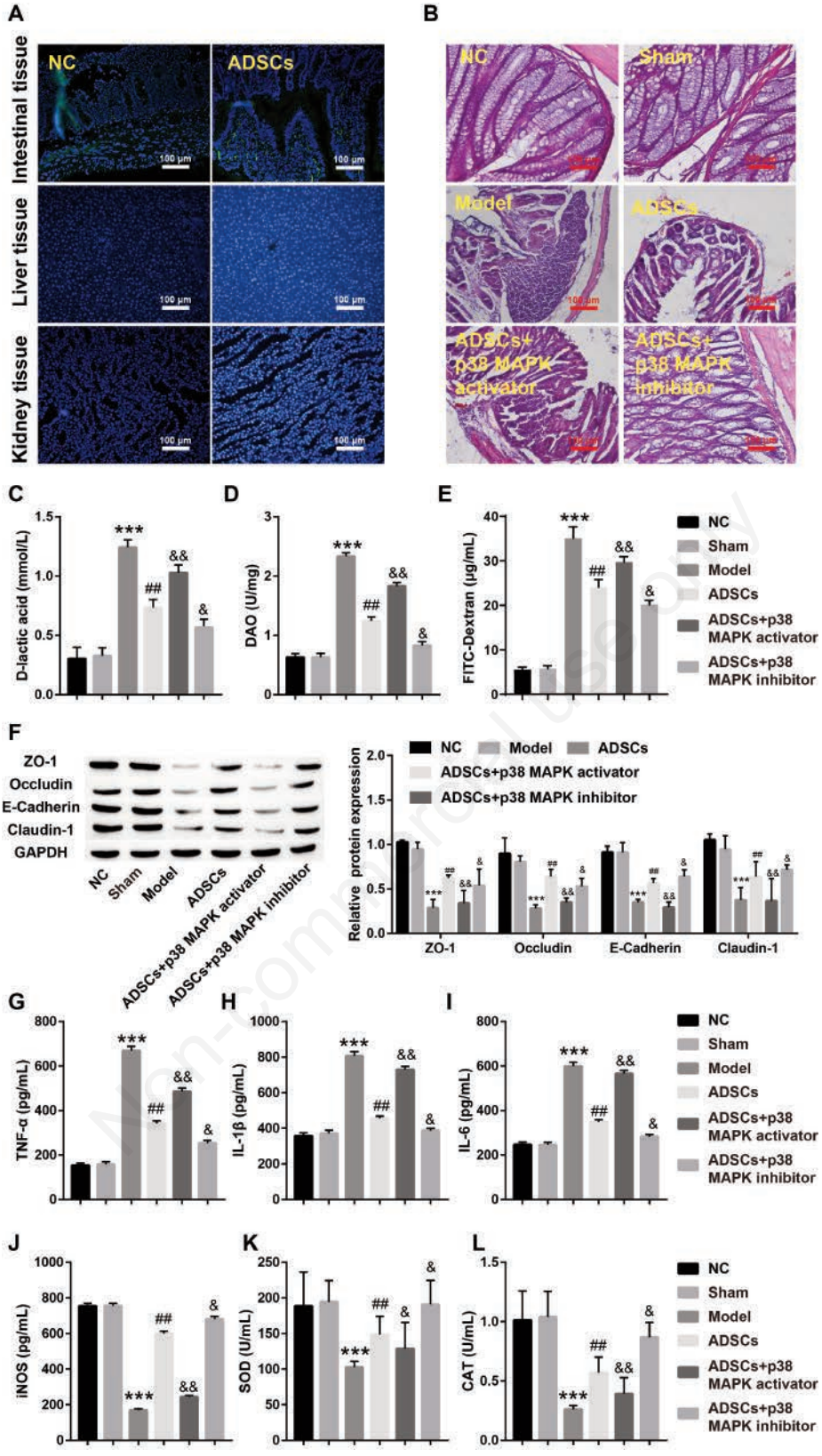

Figure 7. The recruitment of ADSCs to intestinal tissue alleviates intestinal barrier damage by suppressing p38 MAPK. **A**) The homing effect of ADSCs was observed by fluorescence localization. **B**) Intestinal barrier tissue was observed by H&E staining. **C-E**) The levels of D-lactate, DAO and endotoxin were determined by kits. **F**) Tight junction proteins (ZO-1, Occludin, E-cadherin, and Claudin-1) were detected by Western blot. **G-I**) Inflammatory cytokines (TNF-α, IL-1β and IL-6) were measured by ELISA. **J-L**) Antioxidant enzymes (iNOS, SOD and CAT) were measured by kits. ***p<0.001 *vs* Sham group; ##p<0.01 *vs* Model group; $^{\&}p$<0.05, $^{\&\&}p$<0.01 *vs* ADSCs group. (n=5). The full-length gel and blot images are available in the Supplementary Figure.

itis rats, tyrosine and threonine residues in p38 MAPK are phosphorylated, and the levels of LPS and some inflammatory factors increase, further aggravating the inflammatory reaction.[40] In this study, the levels of phosphorylated p38 MAPK in LPS-stimulated cells were significantly greater than those in normal cells, while ADSCs effectively inhibited the phosphorylation of p38 MAPK. This inhibition of p38 MAPK phosphorylation by ADSCs has a profound impact on other proteins and physiological functions. For example, phosphorylated p38 MAPK is known to upregulate the expression of certain pro-inflammatory factors. When ADSCs inhibit p38 MAPK phosphorylation, this leads to a subsequent decrease in the levels of these pro-inflammatory factors.

Furthermore, a p38 MAPK activator and p38 MAPK inhibitor were used to verify the effect of ADSCs on intestinal barrier damage. These results indicate that the p38 MAPK inhibitor restrained the expression of inflammatory cytokines and oxidative stress-related proteins and inhibited apoptosis in Caco-2 cells treated with LPS. Finally, a rat model of intestinal barrier damage was constructed, and p38 MAPK activators and inhibitors were used to observe the role of p38 MAPK in intestinal barrier repair. ADSCs are more effectively transferred to intestinal tissue than to the kidneys or liver. The levels of D-lactate, DAO and FITC-dextran were significantly increased in the model group, indicating that LPS disrupted the integrity of the intestinal mucosal barrier. In addition, LPS induced fewer tight junction proteins and increased the levels of oxidative stress and inflammation. The effects of LPS on intestinal injury and mucosal permeability were attenuated by ADSCs, whereas activation of the p38 MAPK signaling pathway promoted further damage to the intestinal mucosa.

This study revealed that ADSCs can be recruited to intestinal tissue, where they suppress inflammatory cytokines, oxidative stress and cell apoptosis by limiting p38 MAPK and promoting the expression of tight junction proteins. However, this study has several limitations. Firstly, this work only examined intestinal barrier damage induced by LPS. The mechanisms involved in intestinal barrier damage are complex and varied, and the development and occurrence of other mechanisms should be explored. Secondly, our study primarily explored the inhibitory effects of ADSCs on the p38 MAPK signaling pathway. However, it is important to recognize that ADSCs may influence other pathways, such as the ERK and NF-κB signaling pathways. Previous research suggests that ERK signaling may contribute to intestinal epithelial repair by promoting cell proliferation and survival. Similarly, NF-κB has been identified as a critical regulator of the inflammatory response. Future studies should examine whether ADSCs modulate these or other pathways, potentially providing a more comprehensive understanding of their therapeutic effects. Additionally, our study was limited to LPS-induced models; therefore, broader investigations involving other models of intestinal barrier damage are warranted to validate these findings. Our study focused on investigating the mechanisms by which ADSCs promote intestinal barrier repair through the inhibition of the p38 MAPK signaling pathway. While ADSCs have demonstrated significant therapeutic potential, this study did not include a direct comparison of ADSC efficacy with other treatment modalities for intestinal barrier damage, such as pharmacological agents, nutritional interventions, or other cell-based therapies. At present, we could not identify reports comparing ADSCs with other therapeutic approaches in this specific context. This represents a limitation of the current study and an important area for future research, where a comparative analysis could provide valuable insights into the relative efficacy and mechanisms of different therapeutic strategies. Moreover, further validation is needed for the clinical application of gene-targeted therapeutics in the treatment of intestinal barrier damage.

References

1. Sandoval-Ramirez BA, Catalan U, Pedret A, Valls RM, Motilva MJ, Rubio L, et al. Exploring the effects of phenolic compounds to reduce intestinal damage and improve the intestinal barrier integrity: A systematic review of in vivo animal studies. Clin Nutr 2021;40:1719-32.
2. McKenna ZJ, Gorini PF, Gillum TL, Amorim FT, Deyhle MR, Mermier CM. High-altitude exposures and intestinal barrier dysfunction. Am J Physiol-Reg I 2022;322:R192-203.
3. Cao Z, Mu S, Wang M, Zhang Y, Zou G, Yuan X, et al. Succinate pretreatment attenuates intestinal ischemia-reperfusion injury by inhibiting necroptosis and inflammation via upregulating Klf4. Int Immunopharmacol 2023;120:110425.
4. Scaldaferri F, Pizzoferrato M, Gerardi V, Lopetuso L, Gasbarrini A. The gut barrier: new acquisitions and therapeutic approaches. J Clin Gastroenterol 2012;46 Suppl:S12-7.
5. Liu J, Huang L, Luo M, Xia X. Bacterial translocation in acute pancreatitis. Crit Rev Microbiol 2019;45:539-47.
6. Ono K, Han J. The p38 signal transduction pathway: activation and function. Cell Signal 2000;12:1-13.
7. Henson SM, Lanna A, Riddell NE, Franzese O, Macaulay R, Griffiths SJ, et al. p38 signaling inhibits mTORC1-independent autophagy in senescent human CD8(+) T cells. J Clin Invest 2014;124:4004-16.
8. Li Y, Xu B, Xu M, Chen D, Xiong Y, Lian M, et al. 6-Gingerol protects intestinal barrier from ischemia/reperfusion-induced damage via inhibition of p38 MAPK to NF-kappaB signalling. Pharmacol Res 2017;119:137-48.
9. Xiong W, Huang J, Li X, Zhang Z, Jin M, Wang J, et al. Icariin and its phosphorylated derivatives alleviate intestinal epithelial barrier disruption caused by enterotoxigenic Escherichia coli through modulate p38 MAPK in vivo and in vitro. Faseb J 2020;34:1783-801.
10. Ouyang J, Zhang ZH, Zhou YX, Niu WC, Zhou F, Shen CB, et al. Up-regulation of tight-junction proteins by p38 mitogen-activated protein kinase/p53 inhibition leads to a reduction of injury to the intestinal mucosal barrier in severe acute pancreatitis. Pancreas 2016;45:1136-44.
11. Song Y, You Y, Xu X, Lu J, Huang X, Zhang J, et al. Adipose-derived mesenchymal stem cell-derived exosomes biopotentiated extracellular matrix hydrogels accelerate diabetic wound healing and skin regeneration. Adv Sci 2023;10:e2304023.
12. Jin J, Shi Y, Gong J, Zhao L, Li Y, He Q, et al. Exosome secreted from adipose-derived stem cells attenuates diabetic nephropathy by promoting autophagy flux and inhibiting apoptosis in podocyte. Stem Cell Res Ther 2019;10:95.
13. Nishikawa T, Maeda K, Nakamura M, Yamamura T, Sawada T, Mizutani Y, et al. Filtrated adipose tissue-derived mesenchymal stem cell lysate ameliorates experimental acute colitis in mice. Digest Dis Sci 2021;66:1034-44.
14. Yu H, Yang X, Xiao X, Xu M, Yang Y, Xue C, et al. Human adipose mesenchymal stem cell-derived exosomes protect mice from DSS-induced inflammatory bowel disease by promoting intestinal-stem-cell and epithelial regeneration. Aging Dis 2021;12:1423-37.
15. Wang X, Wang Y, Zhou X, Liu F. Conditioned medium from adipose-derived stem cell inhibits Jurkat cell proliferation through TGF-beta1 and p38/MAPK pathway. Anal Cell Pathol 2019;2019:2107414.
16. Gan L, Zheng L, Yao L, Lei L, Huang Y, Zeng Z, et al. Exosomes from adipose-derived mesenchymal stem cells improve liver fibrosis by regulating the miR-20a-5p/TGFBR2 axis to affect the p38 MAPK/NF-kappaB pathway. Cytokine 2023;172:156386.

17. Li Y, Zhang W, Gao J, Liu J, Wang H, Li J, et al. Adipose tissue-derived stem cells suppress hypertrophic scar fibrosis via the p38/MAPK signaling pathway. Stem Cell Res Ther 2016;7:102.
18. Panaro MA, Carofiglio V, Acquafredda A, Cavallo P, Cianciulli A. Anti-inflammatory effects of resveratrol occur via inhibition of lipopolysaccharide-induced NF-kappaB activation in Caco-2 and SW480 human colon cancer cells. Brit J Nutr 2012;108:1623-32.
19. Bolte LA, Vich VA, Imhann F, Collij V, Gacesa R, Peters V, et al. Long-term dietary patterns are associated with pro-inflammatory and anti-inflammatory features of the gut microbiome. Gut 2021;70:1287-98.
20. Flemming S, Luissint AC, Kusters D, Raya-Sandino A, Fan S, Zhou DW, et al. Desmocollin-2 promotes intestinal mucosal repair by controlling integrin-dependent cell adhesion and migration. Mol Biol Cell 2020;31:407-18.
21. Barichello T, Generoso JS, Singer M, Dal-Pizzol F. Biomarkers for sepsis: more than just fever and leukocytosis-a narrative review. Crit Care 2022;26:14.
22. Ge P, Luo Y, Okoye CS, Chen H, Liu J, Zhang G, et al. Intestinal barrier damage, systemic inflammatory response syndrome, and acute lung injury: A troublesome trio for acute pancreatitis. Biomed Pharmacother 2020;132:110770.
23. Lin Z, Lin D, Lin D. The mechanisms of adipose stem cell-derived exosomes promote wound healing and regeneration. Aesthet Plast Surg 2024;48:2730-7.
24. Ni H, Zhao Y, Ji Y, Shen J, Xiang M, Xie Y. Adipose-derived stem cells contribute to cardiovascular remodeling. Aging (Albany NY) 2019;11:11756-69.
25. Al-Ghadban S, Bunnell BA. Adipose tissue-derived stem cells: immunomodulatory effects and therapeutic potential. Physiology 2020;35:125-33.
26. Im GI. Adipose stem cells and skeletal repair. Histol Histopathol 2013;28:557-64.
27. Shingyochi Y, Orbay H, Mizuno H. Adipose-derived stem cells for wound repair and regeneration. Expert Opin Biol Th 2015;15:1285-92.
28. Liu S, Zhang H, Zhang X, Lu W, Huang X, Xie H, et al. Synergistic angiogenesis promoting effects of extracellular matrix scaffolds and adipose-derived stem cells during wound repair. Tissue Eng Pt A 2011;17:725-39.
29. Bhattacharyya A, Chattopadhyay R, Mitra S, Crowe SE. Oxidative stress: an essential factor in the pathogenesis of gastrointestinal mucosal diseases. Physiol Rev 2014;94:329-54.
30. Yu C, Wang Z, Tan S, Wang Q, Zhou C, Kang X, et al. Chronic kidney disease induced intestinal mucosal barrier damage associated with intestinal oxidative stress injury. Gastroent Res Pract 2016;2016:6720575.
31. Jin Y, Zhai Z, Jia H, Lai J, Si X, Wu Z. Kaempferol attenuates diquat-induced oxidative damage and apoptosis in intestinal porcine epithelial cells. Food Funct 2021;12:6889-99.
32. Zhou Q, Xiang H, Liu H, Qi B, Shi X, Guo W, et al. Emodin alleviates intestinal barrier dysfunction by inhibiting apoptosis and regulating the immune response in severe acute pancreatitis. Pancreas 2021;50:1202-11.
33. Kuo WT, Zuo L, Odenwald MA, Madha S, Singh G, Gurniak CB, et al. The tight junction protein ZO-1 is dispensable for barrier function but critical for effective mucosal repair. Gastroenterology 2021;161:1924-39.
34. Jiang Y, Song J, Xu Y, Liu C, Qian W, Bai T, et al. Piezo1 regulates intestinal epithelial function by affecting the tight junction protein claudin-1 via the ROCK pathway. Life Sci 2021;275:119254.
35. Zhou D, Pan Q, Xin FZ, Zhang RN, He CX, Chen GY, et al. Sodium butyrate attenuates high-fat diet-induced steatohepatitis in mice by improving gut microbiota and gastrointestinal barrier. World J Gastroentero 2017;23:60-75.
36. Zhang C, Zhu H, Jie H, Ding H, Sun H. Arbutin ameliorated ulcerative colitis of mice induced by dextran sodium sulfate (DSS). Bioengineered 2021;12:11707-15.
37. Bai B, Ji Z, Wang F, Qin C, Zhou H, Li D, et al. CTRP12 ameliorates post-myocardial infarction heart failure through down-regulation of cardiac apoptosis, oxidative stress and inflammation by influencing the TAK1-p38 MAPK/JNK pathway. Inflamm Res 2023;72:1375-90.
38. Zhao Y, Wang J, Liu X. TRPV4 induces apoptosis via p38 MAPK in human lung cancer cells. Braz J Med Biol Res 2021;54:e10867.
39. Foerster EG, Mukherjee T, Cabral-Fernandes L, Rocha J, Girardin SE, Philpott DJ. How autophagy controls the intestinal epithelial barrier. Autophagy 2022;18:86-103.
40. Ma TM, Xu N, Ma XD, Bai ZH, Tao X, Yan HC. Moxibustion regulates inflammatory mediators and colonic mucosal barrier in ulcerative colitis rats. World J Gastroenterol 2016;22:2566-75.

Received: 5 November 2024. Accepted: 13 December 2024.

Licensee PAGEPress, Italy
European Journal of Histochemistry 2025; 69:4158
doi:10.4081/ejh.2025.4158

Online Supplementary Figure

Full-length gel and blot images.